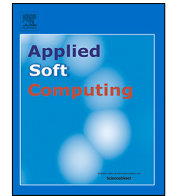




Since January 2020 Elsevier has created a COVID-19 resource centre with free information in English and Mandarin on the novel coronavirus COVID-19. The COVID-19 resource centre is hosted on Elsevier Connect, the company's public news and information website.

Elsevier hereby grants permission to make all its COVID-19-related research that is available on the COVID-19 resource centre - including this research content - immediately available in PubMed Central and other publicly funded repositories, such as the WHO COVID database with rights for unrestricted research re-use and analyses in any form or by any means with acknowledgement of the original source. These permissions are granted for free by Elsevier for as long as the COVID-19 resource centre remains active.



Short-term prediction of COVID-19 spread using grey rolling model optimized by particle swarm optimization

Zeynep Ceylan

Samsun University, Faculty of Engineering, Industrial Engineering Department, 55420, Samsun, Turkey



ARTICLE INFO

Article history:

Received 10 August 2020
 Received in revised form 1 March 2021
 Accepted 4 June 2021
 Available online 9 June 2021

Keywords:

COVID-19
 Prediction
 NARNN
 Grey modelling (1,1)
 Rolling mechanism
 Particle swarm optimization

ABSTRACT

The prediction of the spread of coronavirus disease 2019 (COVID-19) is vital in taking preventive and control measures to reduce human health damage. The Grey Modelling (1,1) is a popular approach used to construct a predictive model with a small-sized dataset. In this study, a hybrid model based on grey prediction and rolling mechanism optimized by particle swarm optimization algorithm (PSO) was applied to create short-term estimates of the total number of confirmed COVID-19 cases for three countries, Germany, Turkey, and the USA. A rolling mechanism that updates data in equal dimensions was applied to improve the forecasting accuracy of the models. The PSO algorithm was used to optimize the Grey Modelling parameters (1,1) to provide more robust and efficient solutions with minimum errors. To compare the accuracy of the predictive models, a nonlinear autoregressive neural network (NARNN) was also developed. According to the analysis results, Grey Rolling Modelling (1,1) optimized by PSO algorithm performs better than the classical Grey Modelling (1,1), Grey Rolling Modelling (1,1), and NARNN models for predicting the total number of confirmed COVID-19 cases. The present study can provide an important basis for countries to allocate health resources and formulate epidemic prevention policies effectively.

© 2021 Elsevier B.V. All rights reserved.

1. Introduction

Millions of people were infected and died due to the new coronavirus disease 2019 (COVID-19), which started at the end of 2019 and affected the whole world in a short time. As a first significant warning against the severe effects of the epidemic, a global pandemic was declared by the World Health Organization (WHO) on March 11, and the world was alarmed [1]. The spread rate, high aggressiveness, and severe damage ability of COVID-19 pose a significant threat to the health and safety of all humanity. While the epidemic has exceeded its peak in many countries, it continues to spread rapidly worldwide. Although the outbreak was brought under control in China, which was the starting point, Europe and America became the new epidemic centres [2].

COVID-19 has become a top priority for researchers worldwide [3,4]. In general, epidemics have a cycle that resembles a bell curve. At first, the epidemic spreads quickly. After a while, it makes a plateau, and then the spread rate (number of infected people) begins to decrease. The time to reach the turning point is related to the dynamics of the countries, and it may differ. These phases of the outbreak are similar to the shape of a bell curve. The form of the bell-curve is related to the policies that countries apply against the epidemic. In countries that strictly

follow the rules and have effective interventions, there will be a broader peak with a lower height. However, in countries that are late to react or implement wrong strategies, a sharp curve will emerge. Of course, this means more infected people, loss of life, and income.

Considering the size and impact of the outbreak, effective healthcare system management is essential to provide fast and accurate treatment for people with COVID-19 symptoms. Thus, it is very important to predict the intensity to be experienced and know the number of cases in advance to provide adequate and timely health care. For this purpose, various studies have been conducted in the literature using different mathematical models to predict the spread of the COVID-19 epidemic [5–7].

Grey prediction models have arisen as a rapid and straightforward modelling and forecasting tool in grey system theory. Grey Modelling (1,1), also abbreviated as GM (1,1), is the simplest primary time-series prediction model in grey system theory. It is the most commonly used grey prediction model in the literature because of its computational efficiency and ability to characterize an unknown system using a limited amount of data [8]. In recent years, the GM (1,1) model has shown satisfactory results in various fields such as environment [9], energy [10], manufacturing [11], transportation [12], and medicine and health [13].

As shown in Table 1, the classical GM (1,1) and its derived models have been used successfully in medicine to predict the

E-mail address: zeynep.ceylan@samsun.edu.tr.

Table 1
Summary of studies on the prediction of epidemic diseases using grey prediction models.

Reference	Disease	Method(s)	Country
Gao et al. [13]	Malaria	GM (1,1)	China
Ding et al. [14]	H1N1	GM (1,1), D-R algorithm	China
Ren et al. [15]	Tuberculosis	GM (1,1), D-R algorithm	US, Germany
Shen et al. [16]	TPF	GM (1,1), DGM	China
Guo et al. [17]	Dysentery and Gonorrhoea	GM (1,1), SMGM (1,1), and Linear Model	China
Zhang et al. [18]	HBV	GM (1,1), GVM, NGBM (1,1), PSO-NNGBM (1,1), and HWES	China
Zhang et al. [19]	Echinococcosis	GM (1,1), PECGM (1,1), FGM (1,1), and SARIMA	China
Yang et al. [20]	TPF	GM (1,1)	China
Wang et al. [21]	HBV	GM (1,1), ARIMA	China
Gao et al. [22]	TPF	GM (1,1), SARIMA	China
Şahin and Şahin [23]	COVID-19	GM (1,1), NGBM (1,1), and FANGBM (1,1)	Italy, UK, and the USA
Luo et al. [24]	COVID-19	GM (1,1), GVM, ARGM (1,1), ONGM (1,1), ENGM (1,1), ARIMA, NGBM (1,1), GRM (1,1), and GERM (1,1, e^{at})	China, Italy, Britain, and Russia
Zhao et al. [25]	COVID-19	Rolling-GVM	China
This study	COVID-19	GM (1,1), Rolling-GM (1,1), Rolling-PSO-GM (1,1), and NARNN	Germany, Turkey, and the USA

H1N1: Influenza A Virus Subtype; HBV: Hepatitis B Virus; TPF: Typhoid and Paratyphoid Fevers; DGM: Discrete Grey Model; SMGM(1,1): GM(1,1) model with self-memory principle; GVM: Grey Verhulst Model; NGBM(1,1): Nonlinear Grey Bernoulli Model; PSO-NNGBM(1,1): Nash Nonlinear Grey Bernoulli Model Optimized by Particle Swarm Optimization; HWES: Holt-Winters Exponential Smoothing; PECGM(1,1): Grey-Periodic Extensional Combinatorial Model; FGM(1,1): Modified Grey Model using Fourier Series; ARIMA: Autoregressive Integrated Moving Average; SARIMA: Seasonal Autoregressive Integrated Moving Average; FANGBM(1,1): Fractional Nonlinear Grey Bernoulli Model; ARGM(1,1): Autoregressive Grey Model; ONGM(1,1): Optimized NGM(1,1,k,c) Model; ENGM(1,1): Exact Nonhomogeneous Grey Model; GRM(1,1): Grey Richards Model; GERM(1,1, e^{at}): Grey Extend Richards Model; Rolling-GVM: Grey Verhulst Models with a Rolling Mechanism; NARNN: Nonlinear Autoregressive Neural Network; Rolling-GM(1,1): GM(1,1) Model with a Rolling Mechanism; Rolling-PSO-GM(1,1): Grey Modelling (1,1) Optimized by Particle Swarm Optimization with a Rolling Mechanism, COVID-19: Coronavirus Disease 2019.

spread of various infectious diseases. For example, Gao et al. (2007) used the GM (1,1) model for forecasting of malaria epidemic situation in Shenzhen Longgang areas [13]. Ding et al. (2011) compared the results of the GM (1,1) model and the D-R algorithm to estimate the trend of H1N1 cases in Mainland China [14]. Ren et al. (2012) analysed tuberculosis incidence rates and deaths in HIV-negative patients in the USA and Germany using the GM (1,1) model [15]. Shen et al. (2013) utilized the grey model to examine typhoid and paratyphoid fever epidemic peaks in China [16]. Guo et al. (2014) used the linear model, the traditional GM (1,1) model, and the GM (1,1) model with the self-memory principle (SMGM(1,1)) to forecast the incidence rates of two notifiable diseases in China [17]. Zhang et al. (2014) used various grey models to forecast the incidence of Hepatitis B in Xinjiang, China [18]. Zhang et al. (2017) applied the different grey models to predict human Echinococcosis spread in Xinjiang, China. They reported that the dynamic epidemic prediction model could identify the future tendency of Echinococcosis outbreak [19].

Yang et al. (2018) applied the GM (1,1) model on the prediction of the incidence trend of typhoid and paratyphoid fevers in Wuhan, China, to help decision-makers to take measures on prevention and control [20]. Wang et al. (2018) compared the success of the GM (1,1) model with the Autoregressive Integrated Moving Average (ARIMA) model for the prediction of hepatitis B in China [21]. Gao et al. (2020) analysed the long-term cumulative incidence of both typhoid and paratyphoid fevers in China using both GM (1,1) and Seasonal Autoregressive Integrated Moving Average (SARIMA) models [22]. Şahin and Şahin (2020) [23], Luo et al. (2020) [24], and Zhao et al. (2020) [25] studied the prediction of cumulative COVID-19 cases using grey prediction models.

As shown in Table 1, the grey prediction model is used as a common tool to predict the spread of different epidemics. This can be attributed to the structure of the GM (1,1) model, which can work efficiently with less data. Despite its wide use, the prediction efficiency of the traditional GM (1,1) model is still being improved [26]. The rolling mechanism developed by Akay and Atak (2007) is one of the most effective methods used to increase the predictive ability of the GM (1,1) model [27]. It includes the use of recent data to handle noisy sequences. Thus, the rolling mechanism was used in this study, as recent data represents the

latest epidemiological trend and characteristic of the epidemic. Besides, the classical GM (1,1) parameters were optimized using Particle Swarm Optimization (PSO), a meta-heuristic algorithm inspired by nature. The main reason for using the PSO algorithm is to provide an advantage for the Rolling-GM (1,1) model due to its quick convergence nature and finding optimal solutions in a reasonable time [28]. The prediction capability of the grey rolling model optimized by the PSO algorithm, abbreviated as Rolling-PSO-GM (1, 1), was also compared with common prediction models such as Nonlinear Autoregressive Neural Network (NARNN), GM (1, 1), and Rolling-GM (1, 1).

The COVID-19 epidemic has reached a peak in many countries. What we know about the virus is much more than the beginning of the outbreak. For this reason, the forecasting studies based on the data at the onset of the epidemic need to be updated and compared. This study aims to accurately estimate the total number of confirmed COVID-19 cases while still experiencing this virus. To the best of the author's knowledge, the Rolling-PSO-GM (1,1) model is used for the first time in estimating the number of COVID-19 cases. Thus, this study is expected to contribute to the literature in this respect. Presenting a case study on Turkey, Germany, and the USA, it is believed that this study can be one of can be the promising alternative and guiding studies for estimating the number of COVID-19 cases for other countries. Furthermore, the results of this study are expected to provide effective guidance in the decision-making process for the prevention and control of epidemics for the governments.

2. Material and methods

2.1. Data collection

In this study, the total confirmed cases of COVID-19 in three countries, Germany, Turkey, the USA, were discussed. The COVID-19 data was taken from the Johns Hopkins University website (<https://github.com/CSSEGISandData/COVID-19>). The 40-day data was divided into two parts: *the in-sample dataset* and *the out-of-sample dataset*. Data from April 26, 2020, to May 30, 2020, were used as an in-sample dataset for model construction. On the other hand, data from April 31, 2020, to June 04, 2020, were used as an out-of-sample dataset to determine how well the developed models perform on the new dataset. All analyses were performed using MATLAB version 2019b software.

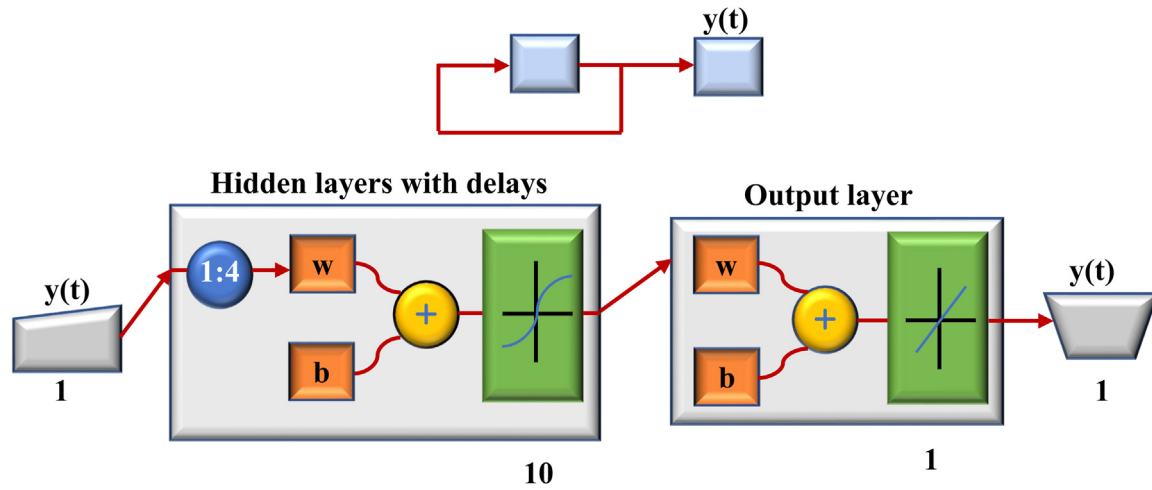


Fig. 1. The structure of the NARNN model.

2.2. Nonlinear autoregressive neural network

The use of linear models makes the problem more burdensome because most of the time-series data include high variability and transient nature [29]. To overcome the limitation of the linear models, nonlinear approaches that recognize time series patterns and nonlinear characteristics of the data are required. Artificial Intelligence (AI) models are frequently used in the literature because they adapt quickly to changes in the system and can successfully predict nonlinear problems [30]. Nonlinear Autoregressive Neural Network (NARNN) is an AI prediction method used to predict next values using historical values of one-dimensional series [31]. It is commonly used in different fields such as wind forecasting [32], global solar radiation forecasting [33], disease prevalence prediction [29], and power prediction [34]. In this study, the NARNN model was built and used for short-term prediction of COVID-19 spread in Germany, Turkey, and the USA. The mathematical representation of the NARNN model can be represented as follows [35]:

$$\hat{y}(t) = k(y(t - 1), y(t - 2), \dots, y(t - d)), \tag{1}$$

where $y(t)$ is the current response, $k(\cdot)$ is the nonlinear function, and it is approximated during the training stage of the network by calculating the optimal weights of the network and the corresponding bias, $(y(t - 1), y(t - 2), \dots, y(t - d))$ are the historical responses, and d is the time delay parameter. In the NARNN model, a closed-loop network is used to perform a multi-step prediction. The output of the closed-loop NARNN model is expressed as follows [35]:

$$\hat{y}(t + p) = k(y(t - 1), y(t - 2), \dots, y(t - d)), \tag{2}$$

where p is the forecast steps in the future. The basic NARNN framework is shown in Fig. 1

The NARNN model has a structure consisting of an input layer, an output layer, and several hidden layers. There are two parameters of the model that need to be specified, i.e., delay order and the number of hidden layer nodes.

2.3. Grey prediction model with rolling mechanism

The grey system theory (GST), dealing with systems having uncertain and incomplete information, was proposed by Julong Deng in the 1980s [36]. The grey prediction in the GST is used to investigate a large amount of unknown information using a small amount of information in a system containing incomplete

data [37,38]. In the grey prediction model GM (n,m), n indicates the order of differential equations, and m indicates the number of variables. In terms of easy calculation, the most commonly used model is the GM (1,1) model. The GM (1,1) model represents the first-order model with a single variable. The GM (1,1) model has many advantages compared to traditional prediction methods because it does not require to know if the prediction variables fit the normal distribution, and also not much statistical samples are necessary [20,39]. Therefore, GM (1,1) model has been used successfully in predicting problems in many disciplines and has achieved very successful results [40]. The grey prediction has three basic operations: the accumulated generating operator (AGO), the inverse accumulating operator (IAGO), and the grey model (GM). The steps of the GM (1,1) model is as follows [41]. **Step 1.** The non-negative row sequence with n samples is presented in Eq. (3).

$$x^{(0)} = (x^{(0)}(1), x^{(0)}(2), x^{(0)}(3), \dots, x^{(0)}(n)) \quad n \geq 4 \tag{3}$$

Monotonically increasing series $x^{(1)}$ is generated by using a one-time accumulating generation operation (1-AGO):

$$x^{(1)} = (x^{(1)}(1), x^{(1)}(2), x^{(1)}(3), \dots, x^{(1)}(n)) \tag{4}$$

where,

$$x^{(1)}(k) = \sum_{i=1}^k x^{(0)}(i); \quad k = 1, 2, 3, \dots, n \tag{5}$$

Step 2. A first-order grey differential equation is formed to obtain GM (1,1) model:

$$x^{(0)}(k) + aZ^{(1)}(k) = b; \quad k = 2, 3, \dots, n \tag{6}$$

where,

$$Z^{(1)}(k) = \gamma x^{(1)}(k) + (1 - \gamma)x^{(1)}(k - 1); \quad k = 2, 3, \dots, n \tag{7}$$

where a and b are called the developing and the driving coefficient, respectively. γ is a dynamic parameter in practical applications and is taken as 0.5 in the original GM (1,1) model. These are two parameters of the GM (1,1) model and can be estimated using the least square method $[a \ b]^T$:

$$\begin{bmatrix} a \\ b \end{bmatrix} = [B^T B]^{-1} B^T Y \tag{8}$$

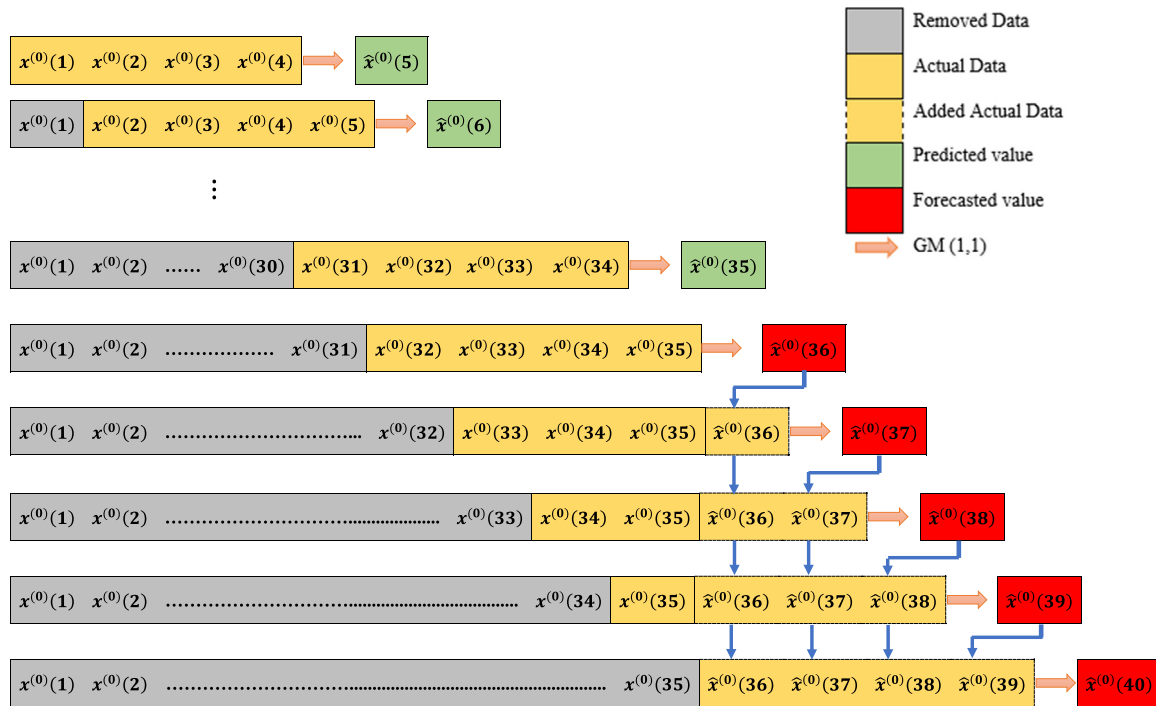


Fig. 2. Forecasting procedure of the Rolling-GM (1,1) model for this study.

where Y is the constant vector, and B is the accumulated matrix.

$$Y = \begin{bmatrix} x^{(0)}(2) \\ x^{(0)}(3) \\ x^{(0)}(4) \\ \vdots \\ \vdots \\ x^{(0)}(n) \end{bmatrix}, \text{ and } B = \begin{bmatrix} -Z^{(1)}(2) & 1 \\ -Z^{(1)}(3) & 1 \\ -Z^{(1)}(4) & 1 \\ \vdots & \\ \vdots & \\ -Z^{(1)}(n) & 1 \end{bmatrix} \quad (9)$$

Step 3. After calculating the a and b coefficients, the GM (1,1) model can be established by solving the differential equation in Eq. (10)

$$x_p^{(0)}(k+1) = x_p^{(1)}(k+1) - x_p^{(1)}(k) = (1 - e^a) \left(x^{(0)} - \frac{b}{a} \right) e^{-ak} \quad (10)$$

$k = 1, 2, 3, \dots, n$

where the initial condition $x^{(1)}(0)$ is taken as $x^{(1)}(1)$.

Typically, in the original GM (1,1) model, all data is used for prediction. However, in the case of chaotic data, it is recommended to use the latest data to improve the prediction accuracy of the GM (1,1) model. To achieve this, the grey prediction with a rolling mechanism (Rolling-GM (1,1)) model based on the rolling steps using the last data, removing the old data for each loop, is used [27]. In Rolling-GM (1,1) model, $x^{(0)}(k+1)$ is forecasted by employing the original GM (1,1) model to $x^{(0)} = x^{(0)}(1), x^{(0)}(2), x^{(0)}(3), \dots, x^{(0)}(n)$ where $k < n$. After the result is found, the forecasting procedure is repeated, but the newly estimated entry $x^{(0)}(k+1)$ is added to at the end of the sequence, and the oldest data $x^{(0)}(1)$ is removed from the data. Next, $x^{(0)} = x^{(0)}(2), x^{(0)}(3), x^{(0)}(4), \dots, x^{(0)}(k+1)$ is used to predict $x^{(0)}(k+2)$. Fig. 2 shows the flow chart of the Rolling-GM (1,1) model for this study [42].

2.4. Parameter optimization

The prediction performance of the GM (1,1) model depends on two parameters calculated in Eq. (8), namely the developing parameter a and the driving coefficient b . In the classical GM (1,1) model, these parameters are calculated by the least-squares estimation method. However, both of these parameters can also be obtained by intelligent optimization algorithms, which can improve the predictive performance of the classical GM (1,1) model. In this study, the optimal values of the a and b coefficients in each rolling period were calculated using the PSO algorithm to increase the prediction accuracy of the COVID-19 spread. The optimization process of the a and b parameters of the GM (1,1) model by PSO algorithm is shown in Fig. 3.

2.5. Particle swarm optimization

The Particle Swarm Optimization (PSO), initially proposed by Kennedy and Eberhart [43], is a population-based optimization algorithm used to achieve the optimal solution, inspired by the social behaviour of birds and fish flocking. PSO algorithm has been successfully applied to a variety of real-world applications because of the computational efficiency in solving complex optimization problems and the rapid convergence to a reasonably good solution [44,45].

In the PSO algorithm, the system starts with a population of random potential solutions, and m particles are generated in the D -dimension solution space randomly. $X_i = (x_i^1, x_i^2, \dots, x_i^D)$ and $V_i = (v_i^1, v_i^2, \dots, v_i^D)$ where $i = 1, 2, 3, \dots, m$, represent the position (direction) and velocity of particles, respectively. Each X position in the flock is scored based on the solution approach to the problem. Personal best (pbest) is the local best of the current generation for each particle; on the other hand, global best (gbest) represents the global best among the local best examples in the current generation. Each particle moves in the direction of its previous best (p_{id}) and the global best (p_{gd}) position in the swarm with a certain velocity to find the gbest position. The following

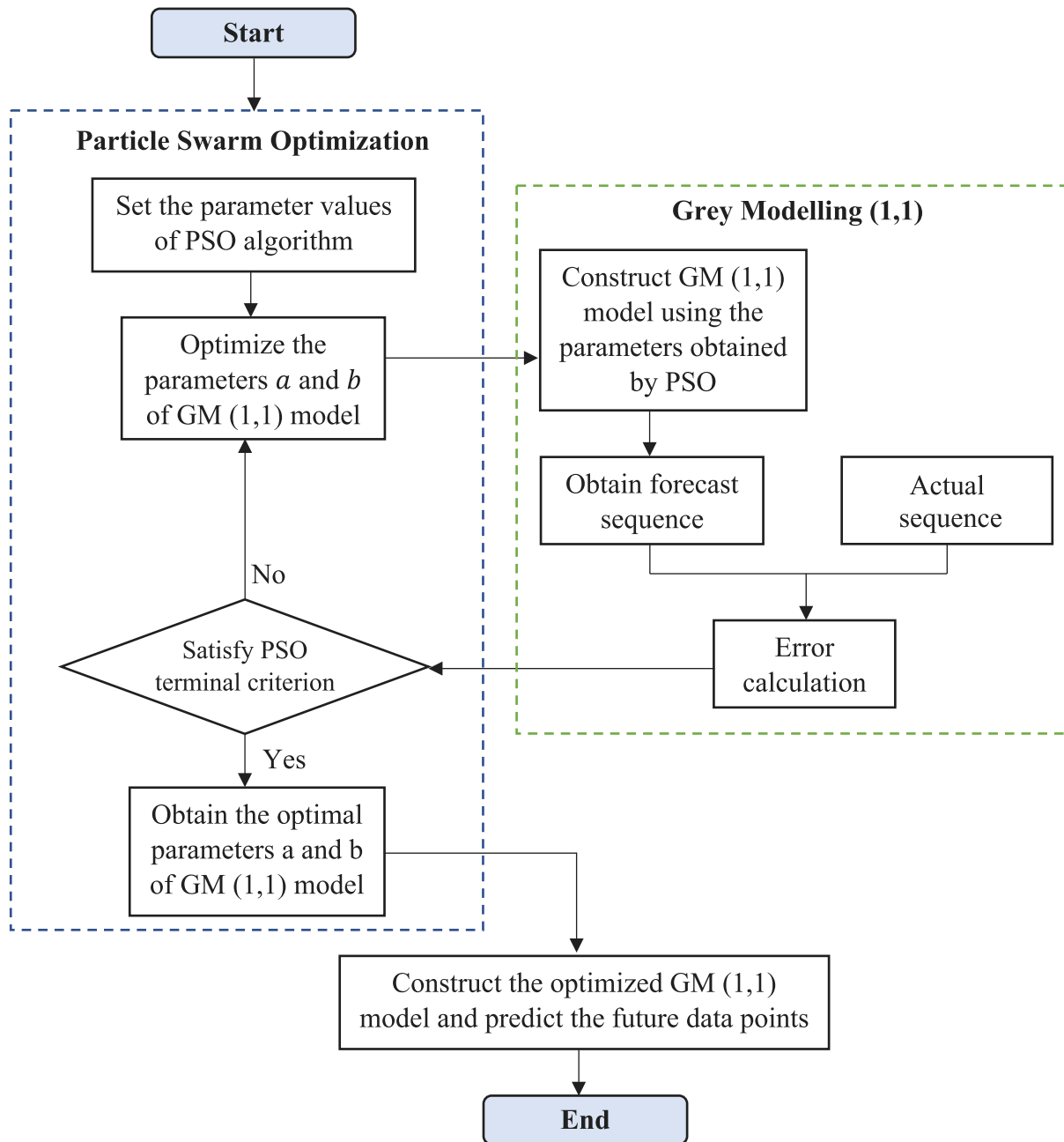


Fig. 3. Flowchart of GM (1,1) model optimized by PSO algorithm.

Eqs. (11) and (12) show how a particle velocity and position are updated [46].

$$v_{id}^{k+1} = wv_{id}^k + c_1r_1(p_{id}^k - x_{id}^k) + c_2r_2(p_{gd}^k - x_{id}^k) \quad (11)$$

$$x_{id}^{k+1} = x_{id}^k + v_{id}^{k+1}; \quad i = 1, 2, 3, \dots, m; d = 1, 2, 3, \dots, D \quad (12)$$

where w represents the inertia weight used to balance the local and global search capabilities of the algorithm, c_1 and c_2 are the acceleration coefficients representing learning behaviour, c_1 enables the particle to benefit from its own experience, c_2 provides the experience of partners' particles in the flock. r_1 and r_2 are uniform random numbers ranging from 0 to 1, k refers to the number of iterations, p_{id}^k is the personal best position of the particle i in the d th dimension, x_{id}^k position and p_{gd}^k is the gbest

position achieved so far in the flock. In the rest of this study, the developed model is abbreviated as Rolling-PSO-GM (1,1). The details of the PSO algorithm are given as follows.

2.6. Performance evaluation metrics

Prediction accuracy is an important criterion for evaluating the performance of a forecasting model. In this study, three metrics were calculated to compare the accuracy and reliability of the models: mean absolute deviation (MAD), root mean square error (RMSE), mean absolute percent error (MAPE%). MAD and RMSE are two metrics of the average magnitude of the forecast errors. MAPE is a general metric considered as a percentage of prediction accuracy. The calculation of MAD, RMSE, and MAPE are given by

Table 2
The parameter values calculated by GM (1,1), Rolling-GM (1,1), and Rolling-PSO-GM (1,1) models.

Country	Date	GM (1,1)		Rolling-GM (1,1)		Rolling-PSO-GM (1,1)	
		a	b	a	b	a	b
Germany	31-May			-0.0027	181,532.5496	-0.0027	181,455.2106
	1-June			-0.0023	182,242.0345	-0.0019	182,380.4666
	2-June	-0.0041	160,780.5359	-0.0026	182,516.5239	-0.0019	182,747.0767
	3-June			-0.0024	183,083.9341	-0.0014	183,382.3125
	4-June			-0.0025	183,457.0084	-0.0016	183,535.6261
Turkey	31-May			-0.0066	159,432.2875	-0.0064	159,452.5876
	1-June			-0.0064	160,557.0853	-0.0062	160,592.7040
	2-June	-0.01036	117,195.8141	-0.0065	161,533.6708	-0.0057	161,825.6768
	3-June			-0.0064	162,620.9347	-0.0059	162,680.5650
	4-June			-0.0065	163,645.0932	-0.0059	163,679.1199
USA	31-May			-0.0137	1,692,244.8785	-0.0135	1,693,002.5918
	1-June			-0.0136	1,716,018.1400	-0.0133	1,717,202.3190
	2-June	-0.0164	1,033,121.5836	-0.0137	1,739,384.9457	-0.0131	1,740,763.5549
	3-June			-0.0136	1,763,534.7679	-0.0127	1,765,423.0989
	4-June			-0.0137	1,787,680.8312	-0.0123	1,789,983.3062

the following Eqs. (13)–(15).

$$MAD = \frac{1}{n} \sum_{k=1}^n |x_k - \hat{x}_k| \tag{13}$$

$$RMSE = \sqrt{\frac{\sum_{k=1}^n (\hat{x}_k - x_k)^2}{n}} \tag{14}$$

$$MAPE = \frac{100\%}{n} \sum_{k=1}^n \left| \frac{x_k - \hat{x}_k}{x_k} \right| \tag{15}$$

where n is the number of observations, x_k and \hat{x}_k are actual and predicted data at time k , respectively. It is known that the model with the lowest MAD, MAPE, and RMSE values means better performance.

3. Results

The classic GM (1,1), Rolling-GM (1,1), NARNN models were employed to verify the effectiveness of the Rolling-PSO-GM (1,1) model in estimating the number of confirmed COVID-19 cases in Germany, Turkey, and the USA. In models with a rolling mechanism, a small value of k is preferred for the rolling if a prediction series includes a significant versatility [27]. In this case, data from the last four periods ($x_{k-4}^0, x_{k-3}^0, x_{k-2}^0$, and x_{k-1}^0) is selected to forecast x_k^0 ($k \geq 5$) point. Therefore, the rolling mechanism in this study was built by selecting the last four days of cumulative COVID-19 cases data. That is, the number of the total confirmed COVID-19 cases for each fifth day is calculated based on the total confirmed data of the previous four days. For example, the total number of COVID-19 cases on April 30 is estimated using data from April 26, 2020, to April 29, 2020. Thus, a and b parameter values in the Rolling-GM (1, 1) model change at each rolling stage.

On the other hand, the NARNN model was implemented using the Neural Network Toolbox in MATLAB version 2019b software. The 35-day dataset was divided into three main subsets: training (70%~25 data), validation (15%~5 data), and test set (15%~5 data). The delay parameter was set to four to compare the NARNN model results with the grey rolling models. Also, the NARNN model was run five times with a single hidden layer with ten neurons. The traditional Levenberg–Marquardt backpropagation algorithm was used to train the model. This algorithm was chosen because it is known as the fastest backpropagation training algorithm in the literature [29].

For the classical GM (1, 1) model, all COVID-19 data from April 26 to May 30, 2020, was used for the inputs of the grey model,

Table 3
The initial parameters of the PSO algorithm.

Parameter	Value
Maximum number of iterations (epochs) to train	2000
Maximum inertia weight, w_{max}	0.8
Minimum inertia weight, w_{min}	0.1
Acceleration coefficients, c_1, c_2	1
Number of particles	70
The maximum velocity	2
Minimum global error gradient	10^{-25}

and then the fixed values of parameters a and b are calculated. For Rolling-PSO-GM (1,1) model, the optimum values of the a and b parameters were obtained by the PSO algorithm at each rolling stage. Table 2 shows the parameters calculated by the three grey prediction models.

According to the PSO operations steps, the parameters of the PSO algorithm are set as follows: In Eq. (11), c_1 and c_2 , cognitive and social acceleration coefficients, respectively, are adjusted small ($c_1 = c_2 = 1$) to avoid missing the optimal solution. Besides, the maximum inertia weight was determined as 0.8 based on the study by Shi and Eberhart [32]. The maximum iteration number (T_{max}) is set to 2000. All initial parameter values of PSO are given in Table 3.

Table 4 shows the forecasting values of NARNN, GM (1,1), Rolling GM (1,1), and Rolling-PSO-GM (1,1) models used to predict the spread of COVID-19 in countries. To directly compare the performance of classical GM (1,1) with rolling-based forecasting models, the values from April 26 to April 29, 2020, were not taken into account.

As seen in Table 4, the Rolling-GM (1,1) and Rolling-PSO-GM (1,1) models outperform the original GM (1, 1) model for all countries. On the other hand, in terms of prediction errors, the NARNN achieved better prediction results than the classical GM (1, 1) model. However, it performed worse than the Rolling-GM (1, 1) and Rolling-PSO-GM (1, 1) models. The main reason for this may be that the rolling-based prediction models have a mechanism that updates the data at each rolling stage. It is seen that the PSO algorithm has significantly improved the prediction performance of the Rolling-GM (1,1) model in both model building and model testing stages. This shows that optimizing the a and b parameters can improve the prediction accuracy of the grey model. Fig. 4 presents the forecasting results of the cumulative cases of COVID-19 for Germany, Turkey, and the USA using Rolling-PSO-GM (1,1) model, respectively. There appears to

Table 4
Comparison of reported and predicted COVID-19 cases for the countries.

Date	Germany					Turkey					USA				
	Actual	NARNN	GM (1,1)	Rolling-GM (1,1)	Rolling-PSO-GM (1,1)	Actual	NARNN	GM (1,1)	Rolling-GM (1,1)	Rolling-PSO-GM (1,1)	Actual	NARNN	GM (1,1)	Rolling-GM (1,1)	Rolling-PSO-GM (1,1)
In-sample															
26-Apr	157,770					110,130					971,078				
27-Apr	158,758					112,261					994,265				
28-Apr	159,912					114,653					1,018,926				
29-Apr	161,539					117,589					1,046,737				
30-Apr	163,009	162,819	163,748	162,871	162,948	120,204	120,534	122,709	120,265	120,347	1,076,224	1,099,297	1,111,092	1,073,548	1,074,002
01-May	164,077	163,988	164,418	164,607	164,559	122,392	122,753	123,987	123,135	123,079	1,110,464	1,121,550	1,129,477	1,105,854	1,106,259
02-May	164,967	164,743	165,091	165,428	165,361	124,375	124,762	125,279	124,938	124,867	1,138,228	1,148,564	1,148,166	1,143,081	1,143,768
03-May	165,664	165,485	165,767	165,985	165,951	126,045	126,496	126,584	126,550	126,520	1,162,685	1,171,283	1,167,164	1,171,625	1,170,557
04-May	166,152	166,169	166,445	166,495	166,525	127,659	128,151	127,902	127,965	127,912	1,186,067	1,193,261	1,186,477	1,190,273	1,189,709
05-May	167,007	166,914	167,126	166,782	166,857	129,491	130,035	129,235	129,344	129,279	1,210,577	1,216,569	1,206,109	1,210,939	1,210,653
06-May	168,162	168,150	167,810	167,622	167,683	131,744	132,085	130,581	131,216	131,239	1,235,666	1,240,133	1,226,066	1,235,110	1,235,451
07-May	169,430	169,512	168,496	169,127	169,135	133,721	134,285	131,941	133,770	133,835	1,263,402	1,263,741	1,246,353	1,261,179	1,261,608
08-May	170,588	170,643	169,186	170,637	170,622	135,569	136,112	133,316	135,934	135,888	1,290,151	1,290,387	1,266,976	1,290,288	1,290,851
09-May	171,324	171,341	169,878	171,833	171,792	137,115	137,729	134,704	137,546	137,503	1,315,099	1,315,525	1,287,941	1,318,484	1,318,084
10-May	171,879	170,715	170,573	172,349	172,279	138,657	139,104	136,108	138,895	138,844	1,333,970	1,338,717	1,309,252	1,342,058	1,341,652
11-May	172,576	170,637	171,271	172,558	172,564	139,771	140,183	137,525	140,229	140,101	1,353,397	1,355,104	1,330,915	1,357,438	1,356,434
12-May	173,171	173,191	171,971	173,182	173,210	141,475	141,887	138,958	141,189	141,118	1,376,122	1,375,093	1,352,938	1,372,892	1,373,339
13-May	174,098	174,085	172,675	173,838	173,870	143,114	142,757	140,406	142,810	142,905	1,397,085	1,400,335	1,375,324	1,397,186	1,397,695
14-May	174,478	174,480	173,382	174,809	174,850	144,749	144,552	141,868	144,827	144,754	1,424,243	1,419,663	1,398,081	1,419,764	1,420,215
15-May	175,233	175,264	174,091	175,226	175,135	146,457	146,889	143,346	146,416	146,433	1,449,498	1,448,977	1,421,215	1,447,964	1,448,931
16-May	175,752	175,776	174,803	175,741	175,803	148,067	148,427	144,839	148,147	148,001	1,473,514	1,472,656	1,444,731	1,476,775	1,476,611
17-May	176,369	175,943	175,519	176,432	176,406	149,435	149,685	146,348	149,772	149,698	1,491,829	1,493,201	1,468,637	1,499,013	1,498,270
18-May	176,551	176,552	176,237	176,924	176,732	150,593	150,741	147,873	150,987	150,927	1,513,816	1,508,073	1,492,938	1,514,400	1,513,456
19-May	177,778	175,809	176,958	177,024	176,952	151,615	151,572	149,413	151,907	151,860	1,534,871	1,532,351	1,517,641	1,533,803	1,534,378
20-May	178,473	176,656	177,682	178,314	178,487	152,587	152,462	150,969	152,740	152,664	1,557,933	1,556,752	1,542,753	1,557,028	1,557,203
21-May	179,021	179,019	178,409	179,530	179,442	153,548	153,435	152,542	153,603	153,565	1,583,798	1,578,484	1,568,280	1,580,169	1,581,012
22-May	179,710	180,489	179,139	179,670	179,701	154,500	154,444	154,131	154,526	154,481	1,607,109	1,606,756	1,594,230	1,608,418	1,608,114
23-May	179,986	179,994	179,872	180,309	180,256	155,686	155,437	155,737	155,467	155,550	1,628,212	1,628,082	1,620,609	1,632,715	1,632,168
24-May	180,328	180,348	180,608	180,539	180,470	156,827	156,407	157,359	156,728	156,796	1,648,158	1,646,710	1,647,425	1,651,264	1,650,785
25-May	180,600	180,597	181,347	180,627	180,594	157,814	157,503	158,998	158,012	157,874	1,666,505	1,666,766	1,674,684	1,669,281	1,668,453
26-May	181,200	180,716	182,089	180,919	181,039	158,762	158,331	160,655	158,915	158,876	1,685,956	1,685,503	1,702,394	1,686,265	1,686,034
27-May	181,524	181,558	182,834	181,583	181,601	159,797	159,416	162,328	159,745	159,777	1,704,489	1,706,408	1,730,563	1,705,015	1,704,499
28-May	182,196	182,195	183,582	182,034	182,052	160,979	160,550	164,019	160,784	160,897	1,727,357	1,726,176	1,759,198	1,723,970	1,725,182
29-May	182,922	182,823	184,333	182,638	182,700	162,120	161,517	165,728	162,076	162,117	1,751,612	1,750,280	1,788,307	1,747,751	1,748,457
30-May	183,189	183,264	185,087	183,616	183,367	163,103	162,359	167,454	163,202	163,172	1,775,428	1,774,423	1,817,898	1,775,458	1,775,591
Out-of-sample															
31-May	183,410	183,538	185,844	183,764	183,688	163,942	163,093	169,199	164,202	164,139	1,794,465	1,793,849	1,847,978	1,800,058	1,799,322
01-Jun	183,594	183,421	186,605	184,135	183,959	164,769	164,006	170,961	165,234	165,096	1,811,393	1,806,855	1,878,556	1,824,673	1,823,222
02-Jun	183,879	183,223	187,368	184,644	184,289	165,555	164,579	172,742	166,322	166,023	1,832,782	1,814,934	1,909,639	1,849,832	1,846,742
03-Jun	184,121	183,057	188,135	185,063	184,500	166,422	167,017	174,542	167,384	167,062	1,852,788	1,820,198	1,941,237	1,875,169	1,869,405
04-Jun	184,472	182,724	188,904	185,544	184,824	167,410	165,874	176,360	168,474	168,042	1,874,156	1,823,506	1,973,358	1,900,935	1,891,680

be good agreement between the reported confirmed cases and the predicted cases.

From Table 5, it is seen that the lowest MAD, RMSE, and MAPE (%) values of the Rolling-PSO-GM (1,1) model for Germany are 222.935, 292.748, and 0.129% in the sample dataset and 356.800, 359.487, and 0.194% in the out-of-sample dataset, respectively. It also performs best with the values of MAD = 201.161, RMSE = 266.677, and MAPE = 0.148% in the sample dataset and MAD = 452.800, RMSE = 484.517, and MAPE = 0.273% in the out-of-sample dataset of Turkey. Similarly, it has the best performance for the USA with the values MAD = 2484.806, RMSE = 3292.779, and MAPE = 0.184% in the sample dataset and MAD = 12957.400, RMSE = 13723.065, and MAPE = 0.703% in the out-of-sample dataset. Clearly, the analysis results confirm that the Rolling-PSO-GM (1,1) is more accurate and provides a significant improvement over the NARNN, traditional GM (1,1), and Rolling-GM (1,1) models.

4. Discussion

The grey system theory requires only a limited number of data to understand the behaviour of unknown systems that differ from other time-series methods. The grey prediction models are widely used for short-term prediction due to the simple calculation ability and higher predictive accuracy. In recent years, grey modelling (1,1) has become increasingly popular in both medicine and public health research. Therefore, in this study, a hybrid model based on grey modelling (1,1) and rolling mechanism optimized by the PSO was used for short-term prediction of COVID-19 spread.

The study results can give information about the estimated number of COVID-19 cases that may occur in the next few days. Since the outbreak started on different dates in different countries, viewing the curve of each country allows us to compare countries more easily. Comparisons between countries can provide preliminary information about where and how the pandemic grew at any given time.

According to results obtained by the Rolling-PSO-GM (1,1) model, the number of confirmed new cases is expected to be an average of 303, 988, and 23250 cases in the next five days (31 May-4 June) for Germany, Turkey, and the USA, respectively. Germany is one of the first countries to develop a reflex against the epidemic, and it has seen a consistent drop in new cases. On the other hand, the total number of COVID-19 continues to increase in the USA, where COVID-19 causes approximately 112,000 deaths, respectively. The country's health system is struggling to cope with the epidemic. The estimates indicate that the current trend is far behind Germany and Turkey. In all three countries, comprehensive prevention and control are required to be maintained and strengthened to reduce the spread of COVID-19.

The present study should be interpreted in light of some limitations. The used data in this study was taken from the official website of Johns Hopkins University. It includes positive cases are that have been confirmed by the state, national or local labs. However, it is difficult to estimate the actual spread of COVID-19 with this information. Because it is more accurate and reliable to say that there are more cases in these countries that have not yet been detected. Thus, it was assumed that the report data in this study might be slightly less than the actual number of cases of COVID-19.

5. Conclusion

There is limited data on the growth trajectory of the COVID-19 outbreak. Besides, the epidemiological features of the new coronavirus are not fully disclosed. Therefore, the prediction of the COVID-19 spread is essential in that it gives an idea of what might happen next days. Public health professionals and policymakers need estimates when making important decisions. These decisions include how to best utilize resources within a health system, which social distancing measures to implement, and what other measures can be taken to reduce the impact

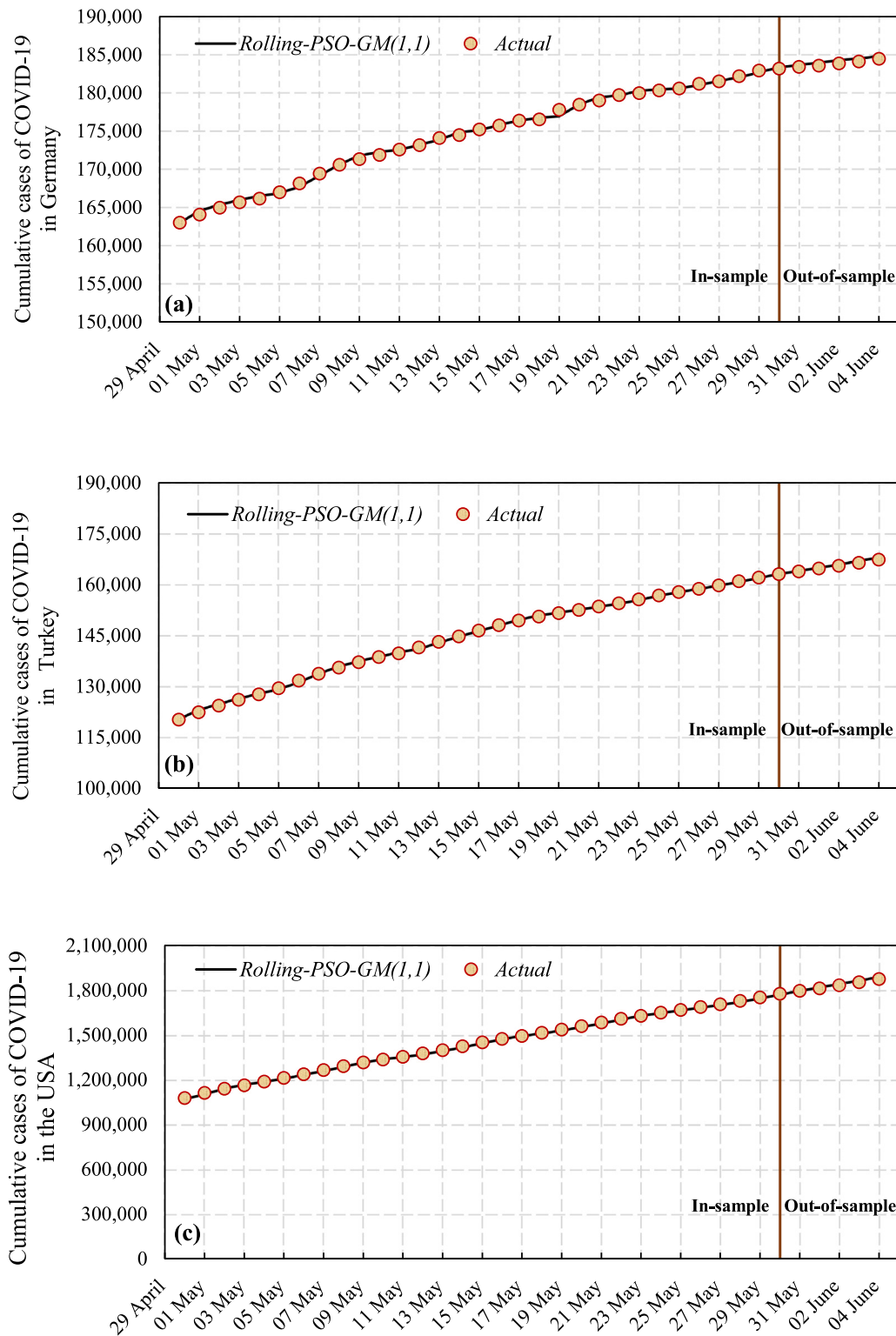


Fig. 4. Actual and predicted values of COVID-19 data in (a) Germany, (b) Turkey, and (c) the USA.

of COVID-19. The forecasts provide preliminary information that shows what might happen in the coming days and whether preventive measures are working. However, traditional methods show limitations such as large amounts of statistical data and a structural system requirement. These pose a significant challenge for researchers to predict the spread of COVID-19 accurately. To overcome the problem, the grey system theory was adopted in predicting the spread of COVID-19 in this study.

The GM (1,1), Rolling-GM (1,1), and Rolling-PSO-GM (1,1) models were used to predict the cumulative case number of COVID-19 in Germany, Turkey, and the USA. Besides, the NARNN model, a neural-based forecasting technique, was also implemented to compare the performance of the developed grey models. Analysis results showed that the use of the rolling mechanism and PSO algorithm with the classical GM (1,1) model has significantly improved the prediction accuracy of the COVID-19 spread.

Table 5

The performance evaluation metrics to compare NARNN, GM (1,1), Rolling-GM (1,1), and Rolling-PSO-GM (1,1) models.

Country	Performance criteria	NARNN	GM (1,1)	Rolling- GM (1,1)	Rolling-PSO-GM (1,1)
<i>In-sample (26 April–30 May)</i>					
Germany	MAD	318.355	847.323	264.484	222.935
	RMSE	659.427	977.334	328.544	292.748
	MAPE (%)	0.182	0.482	0.153	0.129
Turkey	MAD	372.484	1970.355	245.129	201.161
	RMSE	407.328	2253.889	304.895	266.677
	MAPE (%)	0.262	1.353	0.177	0.148
USA	MAD	3698.258	19369.065	2898.677	2484.806
	RMSE	5937.719	21968.532	3702.010	3292.779
	MAPE (%)	0.296	1.347	0.212	0.184
<i>Out-of-sample (31 May–4 June)</i>					
Germany	MAD	753.800	3476.000	734.800	356.800
	RMSE	965.841	3547.349	779.714	359.487
	MAPE (%)	0.409	1.889	0.399	0.194
Turkey	MAD	943.800	7141.200	703.600	452.800
	RMSE	996.882	7261.774	765.461	484.517
	MAPE (%)	0.569	4.306	0.424	0.273
USA	MAD	21248.400	77036.800	17016.600	12957.400
	RMSE	28167.551	78671.177	18527.636	13723.065
	MAPE (%)	1.144	4.190	0.922	0.703

Therefore, the Rolling-PSO-GM (1,1) is selected as the best prediction model with having the lowest prediction errors for all countries. However, the Rolling-PSO-GM (1,1) model cannot take into account the economic and social factors affecting the spread of COVID-19. Also, the effect of climate change was ignored for short-term predictions. These disadvantages can be prevented by using the GM (1, n) model, which can be an important research topic in future studies. Besides, in future studies, the parameters of the classical grey prediction model can be optimized using other techniques such as genetic algorithm or the grey wolf optimizer. Thus, the performance of optimization techniques on the short-term prediction of COVID-19 spread can be compared, and different results can be obtained.

Declaration of competing interest

The authors declare that they have no known competing financial interests or personal relationships that could have appeared to influence the work reported in this paper.

Acknowledgement

This research received no specific grant from any funding agency in the public, commercial, or not-for-profit sectors.

References

- [1] C. Sohrabi, Z. Alsafi, N.O. Neill, M. Khan, A. Kerwan, A. Al-jabir, C. Iosifidis, R. Agha, World health organization declares global emergency: A review of the 2019 novel coronavirus (COVID-19), *Int. J. Surg.* 76 (2020) (2019) 71–76, <http://dx.doi.org/10.1016/j.ijssu.2020.02.034>.
- [2] Z. Ceylan, Estimation of COVID-19 prevalence in Italy, Spain, and France, *Sci. Total Environ.* 729 (2020) <http://dx.doi.org/10.1016/j.scitotenv.2020.138817>.
- [3] C. You, Y. Deng, W. Hu, J. Sun, Q. Lin, F. Zhou, C.H. Pang, Y. Zhang, Z. Chen, X.-H. Zhou, Estimation of the time-varying reproduction number of COVID-19 outbreak in China, *Int. J. Hyg. Environ. Health* 228 (2020) 113555, <http://dx.doi.org/10.1016/j.ijheh.2020.113555>.
- [4] Z. Ceylan, Insights into the relationship between weather parameters and COVID-19 outbreak in lombardy, *Int. J. Healthc. Manag.* 14 (1) (2021) 255–263, <http://dx.doi.org/10.1080/20479700.2020.1858394>.
- [5] A. Tomar, N. Gupta, Prediction for the spread of COVID-19 in India and effectiveness of preventive measures, *Sci. Total Environ.* 728 (2020) 138762, <http://dx.doi.org/10.1016/j.scitotenv.2020.138762>.
- [6] Z. Zhao, X. Li, F. Liu, G. Zhu, C. Ma, L. Wang, Prediction of the COVID-19 spread in african countries and implications for prevention and controls: A case study in South Africa, Egypt, Algeria, Nigeria, Senegal and Kenya, *Sci. Total Environ.* 729 (2020) 138959, <http://dx.doi.org/10.1016/j.scitotenv.2020.138959>.
- [7] M. Maleki, M. Reza, D. Wraith, K. Pho, Time series modelling to forecast the confirmed and recovered cases of, *Travel Med. Infect. Dis.* (2020) 101742, <http://dx.doi.org/10.1016/j.tmaid.2020.101742>.
- [8] P.Ä. Zhou, B.W. Ang, K.L. Poh, A trigonometric grey prediction approach to forecasting electricity demand, Vol. 31 (2006) pp. 2839–2847 <http://dx.doi.org/10.1016/j.energy.2005.12.002>.
- [9] M. Xie, L. Wu, B. Li, Z. Li, A novel hybrid multivariate nonlinear grey model for forecasting the traffic-related emissions, *Appl. Math. Model.* 77 (2020) 1242–1254, <http://dx.doi.org/10.1016/j.apm.2019.09.013>.
- [10] S. Ding, K.W. Hipel, Y. Dang, Forecasting China's electricity consumption using a new grey prediction model, *Energy* 149 (2018) 314–328, <http://dx.doi.org/10.1016/j.energy.2018.01.169>.
- [11] C. Chang, D. Li, Y. Huang, C. Chen, A novel gray forecasting model based on the box plot for small manufacturing data sets, *Appl. Math. Comput.* 265 (2015) 400–408, <http://dx.doi.org/10.1016/j.amc.2015.05.006>.
- [12] Y. Wang, X. Chen, Y. Han, S. Guo, Forecast of passenger and freight traffic volume based on elasticity coefficient method and grey model, *Procedia - Soc. Behav. Sci.* 96 (2013) 136–147, <http://dx.doi.org/10.1016/j.sbspro.2013.08.019>.
- [13] S. Gao, J. Liu, R. Zhang, Y. Gen, D. Huang, S. Wu, Establishment and estimation of a GM (1, 1) grey model for forecasting of malaria epidemic situation in shenzhen longgang areas, *J. Pathog. Biol.* 2 (2007) 357–359.
- [14] F. Ding, D.S. Zarlenga, C. Qin, X. Ren, A novel algorithm to define infection tendencies in H1n1 cases in mainland China, *Infect. Genet. Evol.* 11 (2011) 222–226, <http://dx.doi.org/10.1016/j.meegid.2010.09.015>.
- [15] Y. Ren, F. Ding, S. Suo, R. Bu, D.S. Zarlenga, X. Ren, Incidence Rates and Deaths of Tuberculosis in HIV- Negative Patients in the United States and Germany as Analyzed by New Predictive Model for Infection, Vol. 7 (2015) pp. 1–6 <http://dx.doi.org/10.1371/journal.pone.0042055>.
- [16] X. Shen, L. Ou, X. Chen, X. Zhang, X. Tan, The Application of the Grey Disaster Model to Forecast Epidemic Peaks of Typhoid and Paratyphoid Fever in China, Vol. 8 (2013) pp. 1–6 <http://dx.doi.org/10.1371/journal.pone.0060601>.
- [17] X. Guo, S. Liu, L. Wu, L. Tang, Application of a novel grey self-memory coupling model to forecast the incidence rates of two notifiable diseases in China: Dysentery and gonorrhoea, 2014, pp. 1–17, <http://dx.doi.org/10.1371/journal.pone.0115664>.
- [18] L. Zhang, Y. Zheng, K. Wang, X. Zhang, Y. Zheng, An optimized Nash nonlinear grey Bernoulli model based on particle swarm optimization and its application in prediction for the incidence of hepatitis b in xinjiang, China, *Comput. Biol. Med.* 49 (2014) 67–73, <http://dx.doi.org/10.1016/j.compbiomed.2014.02.008>.
- [19] L. Zhang, L. Wang, Y. Zheng, K. Wang, X. Zhang, Y. Zheng, Time prediction models for echinococcosis based on gray system theory and epidemic dynamics, *Int. J. Environ. Res. Public Health* 14 (2017) <http://dx.doi.org/10.3390/ijerph14030262>.
- [20] X. Yang, J. Zou, D. Kong, G. Jiang, The analysis of GM (1, 1) grey model to predict the incidence trend of typhoid and paratyphoid fevers in wuhan city, China, *Medicine (Baltimore)* 97 (2018) e11787, <http://dx.doi.org/10.1097/MD.00000000000011787>.
- [21] Y.-W. Wang, Z.-Z. Shen, Y. Jiang, Comparison of arima and gm(1,1) models for prediction of hepatitis b in China, *PLoS One* 13 (2018) e0201987, <http://dx.doi.org/10.1371/journal.pone.0201987>.

- [22] J. Gao, J. Li, M.W. Id, Time series analysis of cumulative incidences of typhoid and paratyphoid fevers in China using both grey and SARIMA models, 2020, pp. 1–14, <http://dx.doi.org/10.1371/journal.pone.0241217>.
- [23] U. Şahin, T. Şahin, Forecasting the cumulative number of confirmed cases of COVID-19 in Italy, UK and USA using fractional nonlinear grey Bernoulli model, *Chaos Solitons Fractals* 138 (2020) 109948, <http://dx.doi.org/10.1016/j.chaos.2020.109948>.
- [24] X. Luo, H. Duan, K. Xu, A novel grey model based on traditional richards model and its application in COVID-19, *Chaos Solitons Fractals* (2020) 110480, <http://dx.doi.org/10.1016/j.chaos.2020.110480>.
- [25] Y. Zhao, M. Shou, Z. Wang, Prediction of the number of patients infected with COVID-19 based on rolling grey verhulst models, 2020.
- [26] H. Zhao, H. Zhao, S. Guo, Applied sciences using GM (1, 1) optimized by MFO with rolling mechanism to forecast the electricity consumption of, 2016, <http://dx.doi.org/10.3390/app6010020>.
- [27] D. Akay, M. Atak, Grey prediction with rolling mechanism for electricity demand forecasting of Turkey, *Energy* 32 (2007) 1670–1675, <http://dx.doi.org/10.1016/j.energy.2006.11.014>.
- [28] W. Ma, X. Zhu, M. Wang, Forecasting iron ore import and consumption of China using grey model optimized by particle swarm optimization algorithm, Vol. 38 (2013) pp. 613–620.
- [29] A.I. Saba, A.H. Elsheikh, Forecasting the prevalence of COVID-19 outbreak in Egypt using nonlinear autoregressive artificial neural networks, *Process Saf. Environ. Prot.* 141 (2020) 1–8, <http://dx.doi.org/10.1016/j.psep.2020.05.029>.
- [30] Z. Ceylan, B. Sungur, Estimation of coal elemental composition from proximate analysis using machine learning techniques, *Energy Sources A Recover. Util. Environ. Eff.* 42 (2020) 2576–2592.
- [31] K. Benmouiza, A. Cheknane, Small-scale solar radiation forecasting using arma and nonlinear autoregressive neural network models, 2016, pp. 945–958, <http://dx.doi.org/10.1007/s00704-015-1469-z>.
- [32] A. Ahmed, M. Khalid, Multi-step ahead wind forecasting using nonlinear autoregressive neural networks, *Energy Proc.* 134 (2017) 192–204, <http://dx.doi.org/10.1016/j.egypro.2017.09.609>.
- [33] K. Benmouiza, A. Cheknane, Forecasting hourly global solar radiation using hybrid k -means and nonlinear autoregressive neural network models, *Energy Convers. Manag.* 75 (2013) 561–569, <http://dx.doi.org/10.1016/j.enconman.2013.07.003>.
- [34] J.K. Rogier, N. Mohamudally, Forecasting photovoltaic power generation via an IoT network using nonlinear autoregressive neural network, *Procedia Comput. Sci.* 151 (2019) 643–650, <http://dx.doi.org/10.1016/j.procs.2019.04.086>.
- [35] S. Khaleghi, D. Karimi, S.H. Beheshti, S. Hosen, H. Behi, M. Berecibar, J. Van Mierlo, Online health diagnosis of lithium-ion batteries based on nonlinear autoregressive neural network, *Appl. Energy* 282 (2021) 116159, <http://dx.doi.org/10.1016/j.apenergy.2020.116159>.
- [36] J. Deng, Introduction to grey system, *J. Grey Syst.* 1 (1989) 1–24.
- [37] Y. Lin, M.Y. Chen, S. Liu, Theory of grey systems: Capturing uncertainties of grey information, *Kybernetes.* 33 (2004) 196–218, <http://dx.doi.org/10.1108/03684920410514139>.
- [38] S. Ding, N. Xu, J. Ye, W. Zhou, X. Zhang, Estimating chinese energy-related CO2 emissions by employing a novel discrete grey prediction model, *J. Clean. Prod.* 259 (2020) 120793, <http://dx.doi.org/10.1016/j.jclepro.2020.120793>.
- [39] Y.C. Hu, Electricity consumption prediction using a neural-network-based grey forecasting approach, *J. Oper. Res. Soc.* 68 (2017) 1259–1264, <http://dx.doi.org/10.1057/s41274-016-0150-y>.
- [40] W. Wu, X. Ma, Y. Zhang, W. Li, Y. Wang, Science of the total environment a novel conformable fractional nonhomogeneous grey model for forecasting carbon dioxide emissions of BRICS countries, *Sci. Total Environ.* 707 (2020) 135447, <http://dx.doi.org/10.1016/j.scitotenv.2019.135447>.
- [41] S. Liu, Y. Lin, *Grey Information: Theory and Practical Applications*, in: *Advanced Information and Knowledge Processing*, Springer-Verlag, Berlin, Heidelberg, 2005.
- [42] U. Şahin, Forecasting of Turkey's greenhouse gas emissions using linear and nonlinear rolling metabolic grey model based on optimization, *J. Clean. Prod.* 239 (2019) 118079, <http://dx.doi.org/10.1016/j.jclepro.2019.118079>.
- [43] J. Kennedy, R. Eberhart, *Part. Swarm Optim.* (1995) 1942–1948.
- [44] N. Chouikhi, B. Ammar, N. Rokbani, A.M. Alimi, PSO-Based analysis of echo state network parameters for time series forecasting, *Appl. Soft Comput.* J. 55 (2017) 211–225, <http://dx.doi.org/10.1016/j.asoc.2017.01.049>.
- [45] Z. Ceylan, E. Pekel, S. Ceylan, S. Bulkan, Biomass higher heating value prediction analysis by ANFIS, PSO- ANFIS and GA-ANFIS, *Glob. Nest J.* 20 (2018) 589–597.
- [46] B.C. Ervural, Improvement of grey prediction models and their usage for energy demand forecasting, 2019, <http://dx.doi.org/10.3233/JIFS-17794>.